The influence of tube length, radius and chirality on the buckling behavior of single-walled carbon nanotubes filled with copper atoms

2009 J. Phys.: Condens. Matter 21 305301

(http://iopscience.iop.org/0953-8984/21/30/305301)

J. Phys.: Condens. Matter **21** (2009) 305301 (7pp) doi:10.1088/0953-8984/21/30/305301

The influence of tube length, radius and chirality on the buckling behavior of single-walled carbon nanotubes filled with copper atoms

L Wang[1,2], H W Zhang[1,3] and X M Deng[2]

[1] State Key Laboratory of Structural Analysis for Industrial Equipment, Department of Engineering Mechanics, Dalian University of Technology, Dalian 116024, People's Republic of China
[2] Department of Mechanical Engineering, University of South Carolina, Columbia, SC 29208, USA

E-mail: zhanghw@dlut.edu.cn

Received 27 February 2009, in final form 8 June 2009
Published 6 July 2009
Online at stacks.iop.org/JPhysCM/21/305301

Abstract
The buckling behavior of single-walled carbon nanotubes completely filled with copper atoms under uniaxial compression is investigated using molecular dynamics simulations and compared with that modeled by continuum mechanics. The effects of geometrical characteristics, i.e. tube length, radius and chirality, on buckling deformations are explored separately. Results show that the behavior of encapsulated tubes is more complicated than that of empty ones due to the accommodation of the internal metal atoms. There are both similarities and differences between the results obtained by the molecular dynamics method and continuum mechanics. For a group of completely filled (10, 10) tubes with different length, the dependence of the critical strain on the tube length can be roughly divided into four different linear stages and is accompanied by a transition of the buckling mode from local to global. It is the competition between the evolution of the structure of metal atoms and the variation of the tube length that determines the critical strain. There exists a rather wide range of tube radii within which the critical strain has a weak dependence on tube radius, which differs from the observation for empty tubes. As compared with a zigzag tube of the same length and radius, an armchair tube has a lower critical strain but can be easily strengthened with the incorporation of internal metal atoms.

(Some figures in this article are in colour only in the electronic version)

1. Introduction

Recently, much interest has been shown in carbon nanotubes (CNTs) encapsulating with metal atoms. This kind of metal-filled carbon material can provide potential applications in heterogeneous catalysis, nanodevices, electromagnetic wave absorption, high-density magnetic data storage devices and sensors for magnetic force microscopy, etc [1–7]. Furthermore, the external carbon shell can serve as a barrier against oxidation and, consequently, ensures long-term stability of the internal metal core. Up to now, two main kinds of methods have been proposed to fabricate metal-filled CNTs. One is the *in situ* synthesis during the CNT growth, in which the chemical vapor deposition method is the most widely used fabrication route [8]. Both pure metals and alloys [9–18], especially ferromagnetic metals, are introduced into the cavities of CNTs, providing new composite materials with atypical properties. The other fabrication method of metal-encapsulated CNTs is to fill metals into the prepared CNTs by various means, such as electro-deposition [19, 20], wet chemistry [21, 22], capillary suction [23, 24] and plasma ion irradiation [25].

[3] Author to whom any correspondence should be addressed.

As basic issues, the structure and chemical composition of metal-filled CNTs have been investigated using both experimental techniques and atomistic simulations. Research on different properties, such as metal atom arrangement [26–35], absorption [36] and growth mechanisms [17], and structural transition [37–39], has been carried out. The accommodation of nanosized metal species inside CNTs may lead to essential changes in the electronic and magnetic properties of both the tubes and metals. Based on the metal-filled CNTs, some interesting potential applications have been proposed, such as nanoscale switches [40], superconductivity [41] and air-stable p–n junction diodes [42, 43]. It is also confirmed that both the filling ratio [25, 31] and the thickness of the metal nanowire can play key roles in the determination of the electronic and magnetic properties of the filled CNTs. Thermodynamic behaviors, such as the filling process [44], mass transport [45], solidification [26] and diffusion [46, 47] of the metal atoms, and the structural transformation [48–50] of the metal phase, have also attracted much attention in recent years.

Mechanical deformations of a CNT can both strongly affect the electromagnetic or optical properties and directly lead to failure of CNT-based nanodevices. Therefore, it is important to study the mechanical properties of metal-filled tubes under external loads. To date, only a few results on this issue have been reported. The mechanical properties of CNT-reinforced nickel [51] and copper [52] composites, which are fabricated with an innovative electrochemical co-deposition process, were characterized. It was found that these composites are more than three times stronger than pure nickel or copper. An axial buckling behavior of thick multi-walled carbon nanotubes filled with nickel was observed by ion irradiation [53]. Buckling deformations of single-walled carbon nanotubes (SWCNTs) filled with pure metals [54] and alloys [55] under axial compression were studied using the molecular dynamics (MD) simulation method. Results show that the metal-filled CNTs exhibit different buckling deformation modes as compared with their hollow counterparts. To gain a more complete understanding, in the present work, the buckling behavior of SWCNTs completely filled with copper atoms under uniaxial compression is investigated by MD simulations. The effects of tube length, radius and chirality are isolated separately to clarify the dependence of mechanical behavior of filled tubes on each of the geometrical characteristics.

In section 2, simulation details, including interatomic potentials and geometrical models used in this paper, are introduced briefly. Subsequently, the simulation results and discussions are given in section 3. Finally, the main conclusions are summarized.

2. Simulation details

The use of a proper interatomic potential function is vital for obtaining reasonable and accurate results in MD simulations. In this work, the interactions between carbon atoms are modeled by the second-generation reactive empirical bond order potential which has proven to be reliable for describing the interaction between carbon atoms [56]. The interactions between copper atoms are described by the Sutton–Chen potential [57], which has been frequently used to optimize the structures of transition metal clusters. The interactions between metal atoms and CNTs are represented by the 12-6 Lennard-Jones (LJ) potential [57]. The LJ parameters are calculated by the Lorentz–Berthelot rules. All of the required potential parameters for both Cu–Cu and Cu–C interactions can be found in [57]. The velocity Verlet algorithm is chosen to solve the kinetic equation and the Berendsen thermostat scheme is incorporated into the MD simulations to keep the system temperature at a desired value [58]. Several layers of both metal and carbon atoms located near the top and bottom ends of tubes are constrained as boundaries. The top boundary atoms are shifted as a whole along the axis by a small displacement in each load step; then the whole system is relaxed while keeping the ends constrained. The time step is chosen to be 1.0 fs for all runs.

The procedure for the creation of an initial unstrained structure of a copper-filled CNT is as follows. Firstly, copper atoms of a specified number are randomly distributed within a hollow SWCNT with an assigned radius, length and chirality. The system temperature is initially specified at 1300 K and gradually decreased to 0.01 K. Then a free relaxation is carried out for a sufficiently long time to obtain an initial equilibrium structure. The system temperature during both the free relaxation and the loading process is constrained at 0.01 K. A tube is considered completely filled if the length ratio of the internal metal nanowire to the tube is larger than 0.95.

3. Results and discussion

The top views of various initial unstrained structures of copper-filled SWCNTs with different radii are shown in figure 1. The interaction between a CNT and its filled metal atoms restricts the arrangement of the copper atoms and leads to a form of copper atom distribution consisting of a straight single-atom chain and concentric layers. Within a (5, 5) tube only a single atomic chain of copper atoms exists due to the narrow internal space, while in a (8, 8) tube a combined structure of an atom chain and a cylindrical shell is established. With the increase in the tube radius, the number of concentric shells increases with the growing amount of metal atoms in the tube, as shown in figures 1(c) and (e). A straight single atomic chain exists in the cores of (14, 14) and (18, 18) tubes, as shown in figures 1(f) and (h), while four chains coexist in the cavity of the (16, 16) SWCNT, as shown in figure 1(g). As for the (17, 0) zigzag tube, whose radius is close to that of the (10, 10) tube in figure 1(c), the internal metal atoms aggregate in an analogous way with that of the copper atoms confined in the (10, 10) tube, as shown in figure 1(d). On every concentric layer, copper atoms aggregate into several separate helixes spiraling up along the cylindrical shell, as shown in figure 2.

3.1. Effect of tube length

In order to demonstrate the effect of tube length on the tube behavior, simulations have been carried out to see the mechanical responses of a series of completely filled (10, 10)

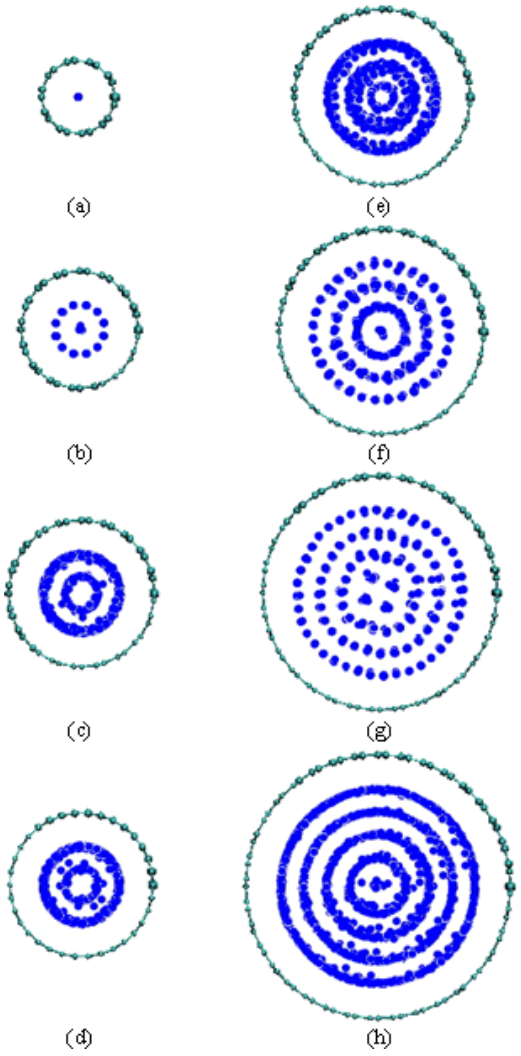

Figure 1. Initial unstrained structures of completely filled SWCNTs with different radii and chirality. (a) (5, 5) tube, (b) (8, 8) tube, (c) (10, 10) tube, (d) (17, 0) tube, (e) (12, 12) tube, (f) (14, 14) tube, (g) (16, 16) tube and (h) (18, 18) tube.

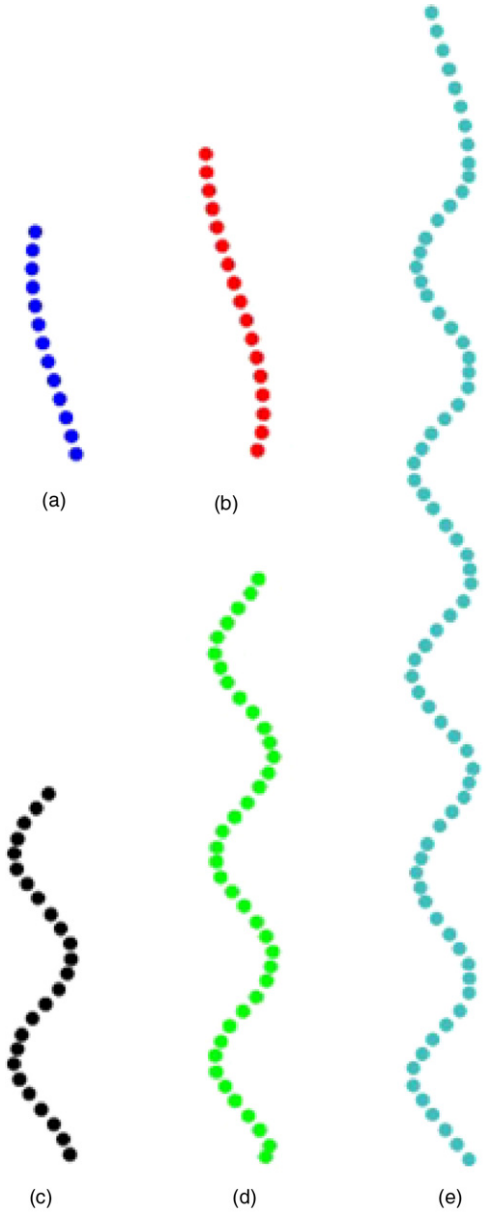

Figure 2. The spiral chain of copper atoms in a tube of length (a) 3 nm, (b) 4 nm, (c) 5 nm, (d) 7.5 nm and (e) 15 nm.

armchair SWCNTs with a tube length ranging from 25.0 to 200.0 Å. Figure 3 is a typical curve of strain energy versus strain for a 5.0 nm-long (10, 10) tube completely filled with copper atoms. Buckling occurs at a critical strain of about 5% when a singularity happens, that is, when the strain energy experiences a sudden drop. In general, a tube that exhibits a larger critical strain is more stable under compression. The linear elastic deformation of the filled tube, prior to buckling, is similar to that of a hollow SWCNT, but the drop in the strain energy for the filled tube at the critical strain is less than that of a corresponding hollow tube [59]. Curves of strain energy versus strain for other tubes in this group are similar to that of the 5.0 nm-long (10, 10) tube and thus are not repeated here.

The relation between the critical strain of a fully filled (10, 10) tube and the tube length is presented in figure 4. It can be seen that the curve can be divided into four linear fragments according to the tube length. In the first stage S1, when the tube is short, the critical strain decreases with the increase in tube length.

In the second stage S2, when the tube length is longer, the critical strain remains constant and is insensitive to the variation of the tube length. In this stage, with the increase of the tube length, helixes of metal atoms are formed and completed, as shown in figures 2(c) and (d), which are more stable than straight chains and hence can help to support more load. Thus, the establishment of spiral chains compensates for the influence of an increased tube length on the critical strain, leading to a segment of horizontal curve.

In the third stage S3, a nearly linear declination of the critical strain with the increase in the tube length is observed. Since the growth of helixes has been completed, as shown in figure 2(e), the effect of tube length retakes dominance and the critical strain continues to decrease with the increase of the tube length. However, the rate of decrease is lower than that in the first stage.

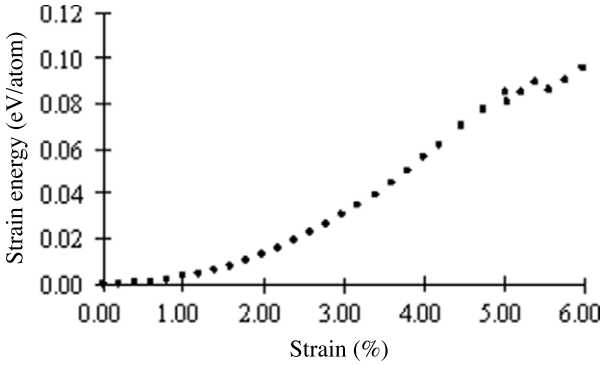

Figure 3. Variation of strain energy with strain during compressive loading of a 5.0 nm-long (10, 10) SWCNT completely filled with copper atoms.

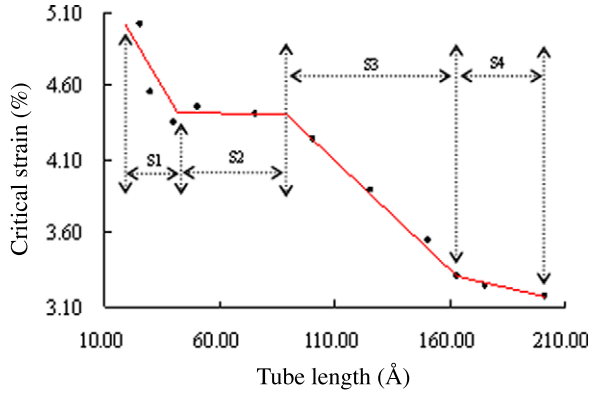

Figure 4. Variation of the critical strain at buckling with tube length, for completely Cu-filled (10, 10) armchair tubes with different lengths. S1–S4 mark different stages.

Finally, in the fourth stage S4, another linear declination is exhibited, which has an even smaller slope than that of the third stage. With a close examination of the buckling configurations, the junction point between the third and fourth stages, with a tube length around 163 Å, is proven to be a critical length from which the buckling mode changes from a local mode to a global mode for an armchair (10, 10) tube.

Two different kinds of buckling modes are presented here for tubes with different lengths. One is the local buckling mode similar to those shown in figure 5, for tubes with a length less than 163 Å, with a straight axis before reaching the critical strain and with lobes on the tube wall on the occurrence of buckling, just like the buckling of thin shells at a macroscale. The other one is the global buckling mode, analogous to those given in figure 6, for tubes with a length equal or larger than 163 Å, in which the tubes keep their circular cross sections and buckle sideways as a whole, similar to the behavior of an Euler rod. It should be noted that the terminologies of 'local buckling' and 'global buckling' are commonly used in the literature [59].

The MD simulation results so far reveal that, for the copper-filled tubes described above, a local buckling mode happens when the tube is short, and a global buckling mode occurs when the tube is long. The critical length for the

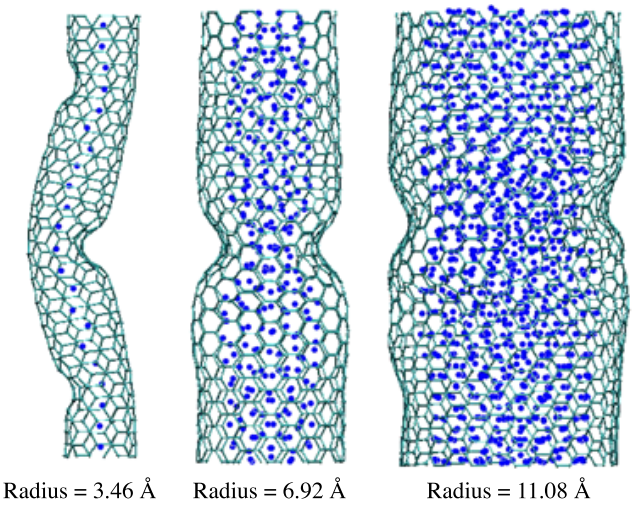

Figure 5. Local buckling modes of 5.0 nm-long (5, 5), (10, 10) and (16, 16) armchair tubes completely filled with copper atoms.

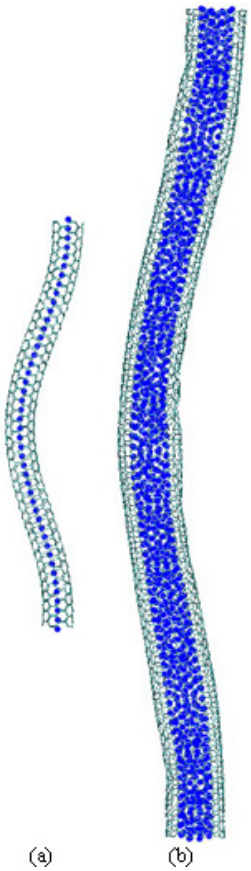

Figure 6. Global buckling modes of long armchair tubes completely filled with copper atoms: (a) 10 nm-long (5, 5) tube and (b) 20 nm-long (10, 10) tube.

transition from a local buckling mode to a global buckling mode is roughly 163 Å for the fully filled (10, 10) armchair tubes described above. Qualitatively, the existence of a transition in buckling mode from short to long tubes is similar to what has been predicted by continuum approaches.

Table 1. The number of copper atoms required to fully fill a 5 nm-long armchair tube.

Tube type	(5, 5)	(6, 6)	(8, 8)	(10, 10)	(12, 12)	(14, 14)	(16, 16)	(18, 18)
Tube radius (Å)	3.46	4.15	5.54	6.92	8.31	9.69	11.08	12.46
Metal atoms	22	64	160	282	500	751	1053	1341

However, there are major differences between MD simulation results and those by continuum approaches when the dependence of the critical strain at buckling on the tube length is concerned. As discussed in [59], according to the continuum mechanics, the critical buckling strain of a thin-shell tube under axial compression is independent of the tube length, which does not coincide with the MD simulation results presented above. Further, it is well known that, according to the continuum mechanics, the critical strain of an Euler rod is inversely proportional to the square of the rod length. However, a nearly linear relationship between the critical strain and the tube length is seen for the global buckling of long tubes, as shown in figure 4. Obviously, the continuum formulation fails to characterize the hybrid structure of metal-filled tubes.

Thus, from the preceding results, it can be concluded that, while the buckling configurations obtained in MD simulations bear similarities to those characterized by continuum mechanics theories, i.e. shorter and longer tubes buckle in local and global buckling modes, respectively, the dependence of the critical strain on the tube length as predicted by MD simulations is different from those by continuum mechanics approaches.

3.2. Effect of tube radius

To examine the effect of tube radius on the tube behavior, a group of completely filled armchair SWCNTs denoted by the index (n, n) $(n = 5, 6, 8, 10, 12, 14, 16, 18)$ are first explored under uniaxial compression. The numbers of copper atoms required to fully fill these tubes are listed in table 1. Tubes in this group are of the same length, i.e. about 5.0 nm, for easy comparison. Figure 5 is a plot of some buckling modes corresponding to (5, 5), (10, 10) and (16, 16) filled tubes with the radii as listed in the figure from left to right, respectively. It can be seen that these are local buckling modes with local collapses on the tube walls, and that the buckling configurations vary with the tube radius. The radius dependence of the critical strain of 5.0 nm-long filled tubes is shown as solid dots in figure 7 (a solid piecewise linear line is fitted to the dots).

It can be seen that, for the 5.0 nm-long tubes, the critical strain first decreases linearly with the increase of the tube radius from 3.46 Å of the (5, 5) tube to 8.31 Å of the (12, 12) tube, and then the critical strain fluctuates in a narrow range around 4.0%. In other words, for these armchair tubes completely filled with metal atoms, there exists a radius range within which no obvious radius dependence of the critical strains is observed. This result differs from the result reported for hollow SWCNTs that the critical strain of hollow tubes decreases monotonically with the increase of the tube radius [59].

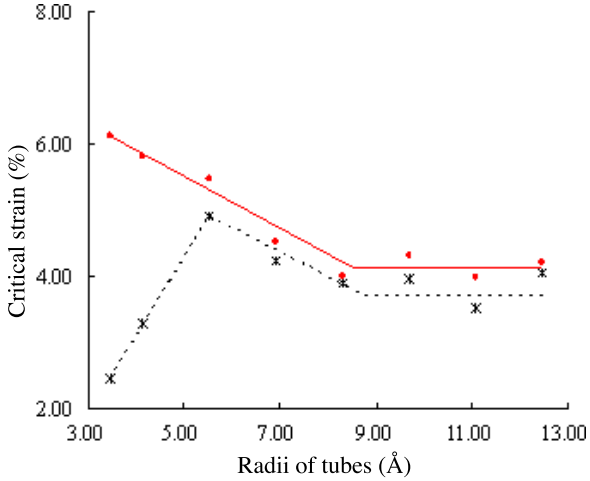

Figure 7. The radius dependence of the critical strain of completely Cu-filled armchair SWCNTs. The solid dots and lines are for 5.0 nm-long tubes, and the crosses and dashed lines are for 10.0 nm-long tubes.

For fully filled tubes in this group, with a fixed length and the same chirality, there are two factors that may influence the critical strain: the tube radius and the constraints exerted by the copper atoms on the tube. As mentioned above, if the internal fillings are absent, the critical strain of a hollow tube tends to drop down with the increase of tube radius. On the other hand, more constraints can enhance the tube buckling strength according to the theory of an Euler rod.

When the internal cavity of a tube is narrow due to a small tube radius, the amount of copper atoms that can fit into the cavity is small. As a consequence, the effect of constraint due to metal atoms is minimal and the effect of radius expansion under compression is dominant, leading to a linearly decreasing variation of the critical strain with tube length, similar to the behavior of hollow tubes.

As the number of metal atoms within the tube grows at a larger radius, the enhancement due to constraints by the metal atoms becomes stronger, which compensates for the negative influence of an increased tube radius, resulting in a fluctuation of the critical strain with tube length. It is the competition between the weakening effect of an increased tube radius and the strengthening effect of the constraints by metal atoms that determines the overall variation of the critical strain.

To further understand the observations made for the 5.0 nm-long tubes, a second group of armchair tubes are considered. This group contains the same tubes except that the tube length is 10.0 nm instead of 5.0 nm. For this group the relationship between the critical strain and the tube radius from MD simulations is shown as crosses and dashed lines in figure 7. It can be seen that the conclusions for the first group

Table 2. The critical strain of empty and completely filled (17, 0) zigzag SWCNTs. Results for counterpart (10, 10) armchair tubes are also included for comparison.

			Critical strains		
Tube type	Radius (Å)	Length (Å)	Empty tubes	Filled tubes	Changes (%)
(17, 0)	6.80	52.20	4.96	5.67	14.31
(10, 10)	6.92	50.23	3.64	4.46	22.53

still hold for the second group except when the tube radius is smaller than about 5.5 Å. For the tubes with a radius smaller than 5.5 Å, the buckling is in a global mode, as shown in figure 6(a) for the 10 nm-long (5, 5) tube, for which the critical strain is much reduced from the corresponding 5 nm-long tube, due to the large slenderness ratio between tube length and radius.

3.3. Effect of tube chirality

The effect of tube chirality on buckling deformation is clarified by simulating the behavior of a fully filled (17, 0) zigzag SWCNT under uniaxial compression. This tube is chosen because its radius and length are nearly equal to those of the (10, 10) tube used in earlier simulations, ensuring the focus on the influence of chirality. The number of internal copper atoms is expected to be and actually close to that in the (10, 10) tube. The initial unstrained structure of the filled (17, 0) tube is also given in figure 1(d). The arrangement of the internal metal atoms is similar to that in the (10, 10) armchair tube in figure 1(c), with two concentric layers and without an atomic chain in the center. The critical strains for empty and completely filled (17, 0) tubes are given in table 2, along with the results of the (10, 10) armchair counterparts for comparison. It can be seen that the completely filled zigzag tube is more stable than the filled armchair tube, which is analogous to the stability rule for empty tubes, as shown in the fourth and fifth columns in table 2. To this end, it is noted that, according to table 2, the strengthening effect due to the encapsulation of copper atoms is stronger (in terms of percentage increase in the critical strain) for the armchair tube than for the zigzag tube. However, with the same radius and length, the completely filled zigzag SWCNT is more stable than its armchair counterpart, while the armchair tube can be enhanced more easily than its zigzag counterpart with the incorporation of internal metal atoms.

4. Conclusions

The buckling behavior of SWCNTs completely filled with copper atoms under uniaxial compression has been studied using MD simulations, with the focus on the effects of tube length, radius and chirality. Results show that the behavior of filled tubes is more complicated than that of empty ones due to the accommodation of the internal metal atoms. There are both similarities and differences between the results obtained by the molecular dynamics method and continuum mechanics.

For a group of completely filled (10, 10) tubes with different lengths, the dependence of the critical strain on tube length can be roughly divided into four different linear stages, and is accompanied by a transition of the buckling mode from local to global at a critical tube length. There is competition between the evolution of the structure of metal atoms and the variation of the tube length on the determination of the critical strain. Local buckling modes with lobes on the tube walls often occur in shorter tubes, which is similar to the buckling of thin shells at the macroscale. In contrast, longer tubes tend to buckle sideways as a whole, just like the deformation of an Euler rod. For a group of filled armchair tubes with the same length but different radii, the critical strain first decreases linearly with the increase of tube radius. Subsequently there exists a rather wide range of tube length within which the critical strain fluctuates and has a weak dependence on tube radius, which differs from the observation for empty tubes, that is, the critical strain decreases monotonically with the increase of tube radius. It is the competition between the effect of tube radius and the constraints exerted by metals on the tube wall that determines the overall variation of the critical strain with tube radius. Compared with a counterpart zigzag tube with the same radius and length, a completely filled armchair tube has a lower critical strain but can be easily strengthened with the incorporation of internal metal atoms.

Acknowledgments

The support of the National Natural Science Foundation of China (10721062, 90715037, 50679013 and 10640420176), the Program for Changjiang Scholars and Innovative Research Team in the University of China (PCSIRT), the 111 Project (no. B08014) and the National Key Basic Research Special Foundation of China (2005CB321704) is gratefully acknowledged. LW thanks the University of South Carolina (USC) for sponsoring a one-year visit to USC and XD thanks the National Natural Science Foundation of China for sponsoring multiple visits to DUT. The authors also would like mention their appreciation of the helpful comments from the referees.

References

[1] Che G, Lakshmi B B, Martin C R and Fisher E R 1999 *Langmuir* **15** 750–8
[2] Svensson K, Olin H and Olsson E 2004 *Phys. Rev. Lett.* **93** 145901
[3] Che R C, Peng L M, Duan X F, Chen Q and Liang X L 2004 *Adv. Mater.* **16** 401–5
[4] Terrones H, López-Urías F, Muñoz-Sandoval E, Rodríguez-Manzo J A, Zamudio A, Elías A L and Torrones M 2006 *Solid State Sci.* **8** 303–20
[5] Winkler A, Mühl T, Menzel S, Kozhuharova-Koseva R, Hampel S, Leonhardt A and Büchner B 2006 *J. Appl. Phys.* **99** 104905
[6] Espinosa E H, Ionescu R, Bittencourt C, Felten A, Erni R, Van Tendeloo G, Pireaux J J and Llobet E 2007 *Thin Solid Films* **515** 8322–7
[7] Costa S, Borowiak-Palen E, Bachmatiuk A, Rümmeli M H, Gemming T and Kaleńczuk R J 2007 *Phys. Status Solidi* b **244** 4315–8

[8] Ajayan P M, Colliex C, Lambert J M, Bernier P, Barbedette L, Tencé M and Stephan O 1994 *Phys. Rev. Lett.* **72** 1722–9
[9] Liang C H, Meng G W, Zhang L D, Shen N F and Zhang X Y 2000 *J. Cryst. Growth* **218** 136–9
[10] Gao X P, Zhang Y, Chen X, Pan G L, Yan J, Wu F, Yuan H T and Song D Y 2004 *Carbon* **42** 47–52
[11] Hampel S, Leonhardt A, Selbmann D, Biedermann K, Elefant D, Müller Ch, Gemming T and Büchner B 2006 *Carbon* **44** 2316–22
[12] Kozhuharova-Koseva R, Elefant D, Hofmann M, Leonhardt A, Mönch I, Ritschel M and Büchner B 2007 *Fuller. Nanotub. Carbon Nanostruct.* **15** 89–97
[13] Kozhuharova-Koseva R, Hofmann M, Leonhardt A, Mönch I, Mühl T, Ritschel M and Büchner B 2007 *Fuller. Nanotub. Carbon Nanostruct.* **15** 135–43
[14] Hayashi Y, Fujita T, Tokunaga T, Kaneko K, Butler T, Rupesinghe N, Carey J D, Silva S R P and Amaratunga G A J 2007 *Diamond Relat. Mater.* **16** 1200–3
[15] Zhang G Y and Wang E G 2003 *Appl. Phys. Lett.* **82** 1926–8
[16] Wang W X, Wang K L, Lv R T, Wei J Q, Zhang X F, Kang F Y, Chang J G, Shu Q K, Wang Y Q and Wu D H 2007 *Carbon* **45** 1127–9
[17] Lv R T, Kang F Y, Wang W X, Wei J Q, Gu J L, Wang K L and Wu D H 2007 *Carbon* **45** 1433–8
[18] Hsin Y L, Hwang K C, Chen F R and Kai J J 2001 *Adv. Mater.* **13** 830–3
[19] Bao J C, Tie C Y, Xu Z, Suo Z Y, Zhou Q F and Hong J M 2002 *Adv. Mater.* **14** 1483–6
[20] Wang X H, Orikasa H, Inokuma N, Yang Q H, Hou P X, Oshima H, Itoh K and Kyotani T 2007 *J. Mater. Chem.* **17** 986–91
[21] Borawiak-Palen E, Mendoza E, Bachmatiuk A, Rummeli M H, Gemming T, Nogues J, Skumryev V, Kalenczuk R J, Pichler T and Silva S R P 2006 *Chem. Phys. Lett.* **421** 129–33
[22] Jain D and Wilhelm R 2007 *Carbon* **45** 602–6
[23] Tan F Y, Fan X B, Zhang G L and Zhang F B 2007 *Mater. Lett.* **61** 1805–8
[24] Jorge J, Flahaut E, Gonzalez-Jimenez F, Gonzalez G, Gonzalez J, Belandria E, Broto J M and Raquet B 2008 *Chem. Phys. Lett.* **457** 347–51
[25] Hatakeyama R and Li Y F 2007 *J. Appl. Phys.* **102** 034309
[26] Kim H and Sigmund W 2005 *Carbon* **43** 1743–8
[27] Golberg D, Mitome M, Müller Ch, Tang C, Leonhardt A and Bando Y 2006 *Acta Mater.* **54** 2567–76
[28] Müller C, Golberg D, Leonhardt A, Hampel S and Büchner B 2006 *Phys. Status Solidi* a **203** 1064–8
[29] Weissmann M, García G, Kiwi M, Ramírez R and Fu C C 2006 *Phys. Rev.* B **73** 125435
[30] Ersen O, Werckmann J, Houllé M, Ledoux M J and Pham-Huu C 2007 *Nano Lett.* **7** 1898–907
[31] Arcidiacono S, Walther J H, Poulikakos D, Passerone D and Koumoutsakos P 2005 *Phys. Rev. Lett.* **94** 105502
[32] Zhang X Q, Li H and Liew K M 2007 *J. Appl. Phys.* **102** 073709
[33] Golberg D, Gu C Z, Bando Y, Mitome M and Tang C C 2005 *Acta Mater.* **53** 1583–93
[34] Shpak A P, Kolesnik S P, Mogilny G S, Petrov Yu N, Sokhatsky V P, Trophimova L N, Shanina B D and Gavriljuk V G 2007 *Acta Mater.* **55** 1769–78
[35] Zhang Q, Qian W Z, Yu H, Wei F and Wen Q 2007 *Appl. Phys.* A **86** 265–9
[36] Sun Y, Yang X B and Ni J 2007 *Phys. Rev.* B **76** 035407
[37] Choi W Y, Kang J W and Hwang H J 2003 *Phys. Rev.* B **68** 193405
[38] Guo Y F, Kong Y, Guo W L and Gao H J 2004 *J. Comput. Theor. Nanosci.* **1** 93–8
[39] Guo Y F and Guo W L 2006 *Nanotechnology* **17** 4726–30
[40] Golberg D, Costa P M F J, Mitome M, Hampel S, Haase D, Mueller C, Leonhardt A and Bando Y 2007 *Adv. Mater.* **19** 1937–42
[41] Tit N and Dharma-wardana M W C 2003 *Europhys. Lett.* **62** 405–11
[42] Li Y F, Hatakeyama R, Shishido J, Kato T and Kaneko T 2007 *Appl. Phys. Lett.* **90** 173127
[43] Kim H S, Kim B K, Kim J J, Lee J O and Park N 2007 *Appl. Phys. Lett.* **91** 153113
[44] Li H Y, Ren X B and Guo X Y 2007 *Chem. Phys. Lett.* **437** 108–11
[45] Schoen P A E, Walther J H, Poulikakos D and Koumoutsakos P 2007 *Appl. Phys. Lett.* **90** 253116
[46] Hwang H J, Kwon O and Kang J W 2004 *Solid State Commun.* **129** 687–90
[47] Zhao M W, Xia Y Y and Mei L M 2005 *Phys. Rev.* B **71** 165413
[48] Karmakar S, Sharma S M, Teredesai P V and Sood A K 2004 *Phys. Rev.* B **69** 165414
[49] Karmakar S, Tyagi P K, Misra D S and Sharma S M 2006 *Phys. Rev.* B **73** 184119
[50] Cheng D J, Wang W C and Huang S P 2007 *J. Phys. Chem.* C **111** 1631–7
[51] Sun Y, Sun J R, Liu M and Chen Q F 2007 *Nanotechnology* **18** 505704
[52] Chai G Y, Sun Y, Sun J R and Chen Q F 2008 *J. Micromech. Microeng.* **18** 035013
[53] Misra A, Tyagi P K, Rai P, Mahopatra D R, Ghatak J, Satyam P V, Avasthi D K and Misra D S 2007 *Phys. Rev.* B **76** 014108
[54] Wang L, Zhang H W, Zhang Z Q, Zheng Y G and Wang J B 2007 *Appl. Phys. Lett.* **91** 051122
[55] Wang L, Zhang H W, Zheng Y G, Wang J B and Zhang Z Q 2008 *J. Appl. Phys.* **103** 083519
[56] Brenner D W, Shenderova O A, Harrison J A, Stuart S J, Ni B and Sinnott S B 2002 *J. Phys.: Condens. Matter* **14** 783–802
[57] Huang S P, Mainardi D S and Balbuena P B 2003 *Surf. Sci.* **545** 163–79
[58] Berendsen H J C, van Gunsteren Postma W F, Di Nola A and Haak J R 1984 *J. Chem. Phys.* **81** 3684–90
[59] Wang Y, Wang X X, Ni X G and Wu H A 2005 *Comput. Mater. Sci.* **32** 141–6